ORIGINAL ARTICLE

Allogeneic haematopoietic cell transplants as dynamical systems: influence of early-term immune milieu on long-term T-cell recovery

Viktoriya Zelikson[1], Roy Sabo[2], Myrna Serrano[3], Younus Aqeel[1], Savannah Ward[1], Taha Al Juhaishi[1], May Aziz[4], Elizabeth Krieger[5], Gary Simmons[1], Catherine Roberts[1], Jason Reed[6], Gregory Buck[2] & Amir Toor[1,7] (ID)

[1]Department of Internal Medicine, Virginia Commonwealth University, Richmond, VA, USA
[2]Department of Biostatistics, Virginia Commonwealth University, Richmond, VA, USA
[3]Department of Microbiology and Immunology, Virginia Commonwealth University, Richmond, VA, USA
[4]Department of Pharmacy, Virginia Commonwealth University, Richmond, VA, USA
[5]Department of Pediatrics, Virginia Commonwealth University, Richmond, VA, USA
[6]Department of Physics, Virginia Commonwealth University, Richmond, VA, USA
[7]Lehigh Valley Topper Cancer Institute, Allentown, PA, USA

Correspondence

A Toor, Transplant and Cellular Therapy Program, Lehigh Valley Topper Cancer Institute, Allentown, PA, USA & Department of Medicine and Pediatrics, Massey Cancer Center, Virginia Commonwealth University, Richmond, VA 23059, USA.
E-mail: amir.toor@lvhn.org

Abstract

Objectives. Immune recovery following haematopoietic cell transplantation (HCT) functions as a dynamical system. Reducing the duration of intense immune suppression and augmenting antigen presentation has the potential to optimise T-cell reconstitution, potentially influencing long-term outcomes. **Methods.** Based on donor-derived T-cell recovery, 26 patients were adaptively randomised between mycophenolate mofetil (MMF) administered for 30-day post-transplant with filgrastim for cytokine support (MMF30 arm, $N = 11$), or MMF given for 15 days with sargramostim (MMF15 arm, $N = 15$). All patients underwent *in vivo* T-cell depletion with 5.1 mg kg^{-1} antithymocyte globulin (administered over 3 days, Day -9 through to Day -7) and received reduced intensity 450 cGy total body irradiation (3 fractions on Day -1 and Day 0). Patients underwent HLA-matched related and unrelated donor haematopoietic cell transplantation (HCT). **Results.** Clinical outcomes were equivalent between the two groups. The MMF15 arm demonstrated superior T-cell, as well as T-cell subset recovery and a trend towards superior T-cell receptor (TCR) diversity in the first month with this difference persisting through the first year. T-cell repertoire recovery was more rapid and sustained, as well as more diverse in the MMF15 arm. **Conclusion.** The long-term superior immune recovery in the MMF15 arm, administered GMCSF, is consistent with a disproportionate impact of early interventions in HCT. Modifying the 'immune-milieu' following allogeneic HCT is feasible and may influence long-term T-cell recovery.

INTRODUCTION

Allogeneic haematopoietic cell transplantation (HCT) is conventionally modelled as a stochastic system, where recipient, donor and disease characteristics determine clinical outcomes.[1] The probabilities of optimal outcomes, such as regimen-related toxicity, graft versus leukaemia (GVL) effect, graft versus host disease (GVHD) and infections are governed by the conditioning intensity, GVHD prophylaxis, disease control and human leukocyte antigen (HLA) matching of donors and recipients. Conventional clinical trial design lends itself to studying the consequences of defined interventions in a limited number of these parameters; for example, comparing myeloablative vs. reduced intensity conditioning (RIC) for transplanting patients with acute myelogenous leukaemia (AML),[2] or the use of bone marrow vs. peripheral blood stem cells (PBSC) for unrelated donor transplantation.[3] This has been a remarkably successful paradigm, which has over the years led to the evolution of the field from a perilous, seldom used option, to a routinely applied therapeutic modality. Nevertheless, at an individual patient level, outcomes remain stochastic with little predictability of complications of therapy in transplant recipients. Close clinical follow-up and laboratory monitoring for variables such as measurable residual disease and chimerism still provide the best tools for early intervention and achieving optimal outcomes.[4] However, these tend to require a considerable lead time to be interpretable and are generally not informative in the early-term post-HCT.

Major causes of treatment failure after an allograft are relapsed malignancy and nonrelapse mortality (NRM), with a reciprocal relationship between conditioning intensity and GVHD prophylaxis for both outcomes. RIC reduces NRM, but relapse risk is higher in some malignancies less susceptible to GVL effects, while intense GVHD prophylaxis may increase infection and relapse risk, and inadequate immune suppression increases GVHD likelihood through the different strata of histocompatibility between donors and recipients. The current state of science is to apply immunosuppression in equal measure across donors with a given level of HLA compatibility.[5] As a consequence considerable variation is observed in immune recovery post-transplant, and subsequently in clinical outcomes.[6] Complex trial design addressing multiple aspects of transplant immunobiology are therefore needed to increase the efficiency with which clinical trials lead to therapy optimisation.

The central role of immune recovery, particularly that of T-cells, in transplant immunobiology has been established through observations such as, relapse prevention in patients with GVHD,[7] relapse treatment with donor lymphocyte infusions[8] and establishment of engraftment with nonmyeloablative conditioning.[9] Previous work has demonstrated that immune reconstitution following HCT has characteristics of a dynamical system; systems that may be modelled with mathematical precision.[10–12] In these studies, lymphocyte and T-cell recovery post-transplant was modelled utilising equations of growth, where cell proliferation occurs as a logistic function of time. This entails, a period of slow initial growth, followed by an exponential proliferation of the immune cell populations with a final steady state being reached with stable counts in the absence of events, such as infections, GVHD or chemotherapy, which would trigger either renewed growth or decline in cell counts. Furthermore, when the T-cell repertoire was examined quantitatively in transplant recipients, using next-generation sequencing (NGS) of the T-cell receptor beta, fractal organisation of T-cell clonal populations was observed with Power laws governing the clonal frequency distribution.[13,14] This clonal hierarchy suggested that growth of T-cell clones is an ordered process, possibly driven by antigen binding affinity among other factors. A parallel series of studies examining transplant donor-recipient whole exomes using NGS identified nonsynonymous polymorphisms in the recipients, which were then used to simulate a donor T-cell response *in silico* and reproduced the power law distribution observed in the clinical studies.[15,16] Further evidence of dynamical behaviour comes from the observation that early interventions have a lasting impact on transplant outcomes, for example the use of post-transplant cyclophosphamide given on Days 3 and 4 post-transplant, which mitigates chronic GVHD many months later.[17–19] Chronic GVHD risk is also mitigated using antithymocyte globulin (ATG), particularly following HLA-matched unrelated donor HCT.[20–22]

However, ATG administration delays T-cell recovery, especially CD4$^+$ helper T-cell reconstitution[23–25] and may impact relapse and viral infection risk. The timing of administration of ATG for *in vivo* T-cell depletion alters the dynamics of T-cell recovery post-transplant and allows superior T-cell recovery if given early in the conditioning regimen.[11,26] Furthermore, given the dynamical systems nature of immune recovery, T-cell reconstitution may be further enhanced by adjustment in the early post-transplant immune milieu, such as intensity of immune suppression and myeloid populations recovering post-transplant.

Post-transplant GVHD prophylaxis in conventional regimens includes a calcineurin inhibitor (CNI) given with a cell cycle active agent such as methotrexate or mycophenolate mofetil (MMF).[27] Methotrexate or mycophenolate mofetil is generally given over a month, marking the period of intense post-transplant immune suppression, generally following immunoablative RIC regimens. The duration of MMF administration derives from clinical trials following the original canine experiments where CNI + MMF was the optimal immune suppression for nonmyeloablative (NMA) conditioning with 2-Gray (Gy) total body irradiation (TBI) and HCT.[28] This concept combined with related work demonstrating engraftment across major histocompatibility antigen barriers with anti-T-cell antibodies[29] formed the basis of an immunoablative, RIC regimen combining 4.5-Gy TBI with early administration of ATG (Day −9 through to Day −7) reported here.[10,24] Aside from the duration of immune suppression, myeloid recovery, specifically monocyte/dendritic cell recovery, may also influence T-cell recovery.[30–32] Granulocyte-macrophage colony stimulating factor (GM-CSF) has an established role in dendritic cell differentiation[33,34] and has been safely utilised following allogeneic HCT.[35] GM-CSF has also been used to augment immune response following HCT and may enhance T-cell-mediated GVL.[36]

Optimal immune response against cancers represents an intersection of multiple factors impacting dendritic cell and T-cell function.[37] Therefore, the adaptively randomised trial reported here tested the combined effect of administering intense post-transplant immune suppression for different duration, as well as the differential impact of post-transplant cytokine therapy in patients conditioned with the reduced intensity ATG and 4.5-Gy TBI regimen (ATG-TBI).[38] T-cell and monocyte recovery results from the two study arms are reported, as are the clinical outcomes.

RESULTS

Clinical outcomes

The two study arms were well-matched for various study variables (Table 1). The median neutrophil engraftment time was shorter (MMF15, Day 14 vs. MMF30, Day 11, $P = 0.0186$) and ANC was higher ($P = 0.0384$) in the MMF30 cohort, in which patients received GSCF. All patients in the study cohort had myeloid engraftment, median granulocyte chimerism was 100% donor-derived at Days 30, 60 and 90; there was one instance of graft failure in the control arm (FET; $P = 0.423$).

With a median follow-up of 35.4 and 32.3 months in the MMF15 and MMF30 arms, respectively, there was a trend towards improved OS in the MMF15 arm (Figure 1). The primary outcome of DLI-free and relapse-free survival was not different between the two groups. Relapse and NRM were similar (Figure 1). Of the MMF15 patients who relapsed, 60% survived, compared with none in the MMF30 arm. DLI were administered for mixed chimerism (MMF15, 1 vs. MMF30, 0), relapse (4 vs. 2), persistent disease (0 vs. 1) and graft failure (0 vs. 1). There was no difference in DLI use between the two study arms (5 vs. 4, $P = 1$).

There was a trend towards increased acute GVHD grade 2–4 in the MMF30 arm and conversely a trend towards increased moderate–severe chronic GVHD in the MMF15 arm (Supplementary figure 1). There was no difference in cumulative incidence of relapse and cGVHD between the two arms (Supplementary figure 2). Individual patient outcomes are given in Supplementary table 1.

Early- and long-term immune reconstitution

T-cell recovery was superior in the MMF15 arm with the T-cell count on Day 30 being significantly higher in the investigational cohort than in the MMF30 (+GCSF) arm (Figures 2–4). Furthermore, this trend was observed beyond Day 180 with the average CD3$^+$ cell count being approximately two times higher in the MMF15 cohort, regardless of donor type. Although the adaptive randomisation was based on ddCD3 cell count on Day 60, with a larger number of patients randomised to the study arm that showed superior ddCD3$^+$ cell recovery, there was no significant difference at Day 60 in any T-cell subset studied, underscoring that superior T-cell recovery over time was not an

Table 1. Patient demographics

Demographics	MMF 15	MMF 30	*P* (FET)
N	15	11	
Age (median)	61.5 (50–68)	56.7 (42–69)	0.25 (Wilcoxon)
Gender (F)	6 (40%)	6 (54.5%)	0.69
KPS (90–100)	5 (33.3%)	3 (27.2%)	1
Disease type (myeloid)	6 (40%)	3 (27.2%)	0.68
AML	5 (30%)	2 (18.2%)	0.66
CLL	4 (26.6%)	1 (9.1%)	0.36
CML	0	1 (9.1%)	0.42
MDS	1 (6.7%)	1 (9.1%)	1
MM	2 (13.3%)	2 (18.2%)	1
NHL	3 (20%)	4 (36.4%)	0.41
HLA match (8/8, 10/10)*	14 (93.3%)	8 (72.7%)	0.27
HLA-MRD	6 (40%)**	2 (18.2%)	0.39
Disease risk index (DRI)			
Low	3	3	1
Intermediate	8	6	1
High	4	2	0.67
Gender mismatch			
M (R) × F (D)	1	1	1
M (R) × M (D)	8	4	0.45
F (R) × M (D)	3	2	1
F (R) × F (D)	3	4	0.4
CMV seropositivity			
+ (R) × + (D)	6	4	1
+ (R) × − (D)	3	1	0.61
− (R) × + (D)	0	3	0.06
− (R) × − (D)	6	3	0.68
Blood type (mismatched)	6	3	0.68
Engraftment time (median)	14	11	0.02 (Wilcoxon)
GCSF- mobilised PBSC	15 (100%)	10 (91%)	0.423
CD34 Dose (10^6) (mean/SD)	4.52 ± 1.71	4.81 ± 2.29	0.86 (Wilcoxon)

artefact of the adaptive randomisation process. $CD3^+/4^+$ and $CD3^+/8^+$ T-cells were also consistently higher in the MMF15 arm, regardless of the donor type. NK cells also showed superior reconstitution in the MMF15 arm (Figure 5); however, B-cell recovery was not different (Figure 6).

Interaction effects between monocyte counts on Day 15 and Day 30 and ddCD3, ddCD4 and ddCD8 counts on Day 30 were significant ($P < 0.0001$) (Supplementary figure 3a–f). Sustained high monocyte counts on both Days 15 and 30 were associated with higher mean T-cell counts. When Day 15 monocyte counts were low, resulting T-cell counts were typically low, regardless of the Day 30 monocyte count and *vice versa*. Consistent with superior T-cell recovery observed in the MMF 15 arm, the gradient of monocyte count between Days 15 and 30, that is the rate of monocyte growth, was higher in this arm where GM-CSF was utilised ($P = 0.005$) (Figure 7). The overall monocyte recovery was not significantly different between the two arms.

Impact of immune cell recovery on clinical outcomes

The effect of T-cell, B-cell and NK-cell reconstitution on clinical outcomes in all trial participants was studied in the combined study population (Supplementary table 2). Higher ddCD3 count on Day 30 was associated with an increased risk of grade 2–4 aGVHD (HR = 1.005, $P = 0.015$). Similarly, ddCD8 count on Day 30 was associated with increased risk of grade 2–4 aGVHD, as well as grade 3–4 aGVHD (aGVHD grade 2–4 HR; 1.008, $P = 0.0007$, grade 3–4 HR; 1.008, $P = 0.04$). Higher ddCD4 cell count on Day 90 was associated with an increased risk of
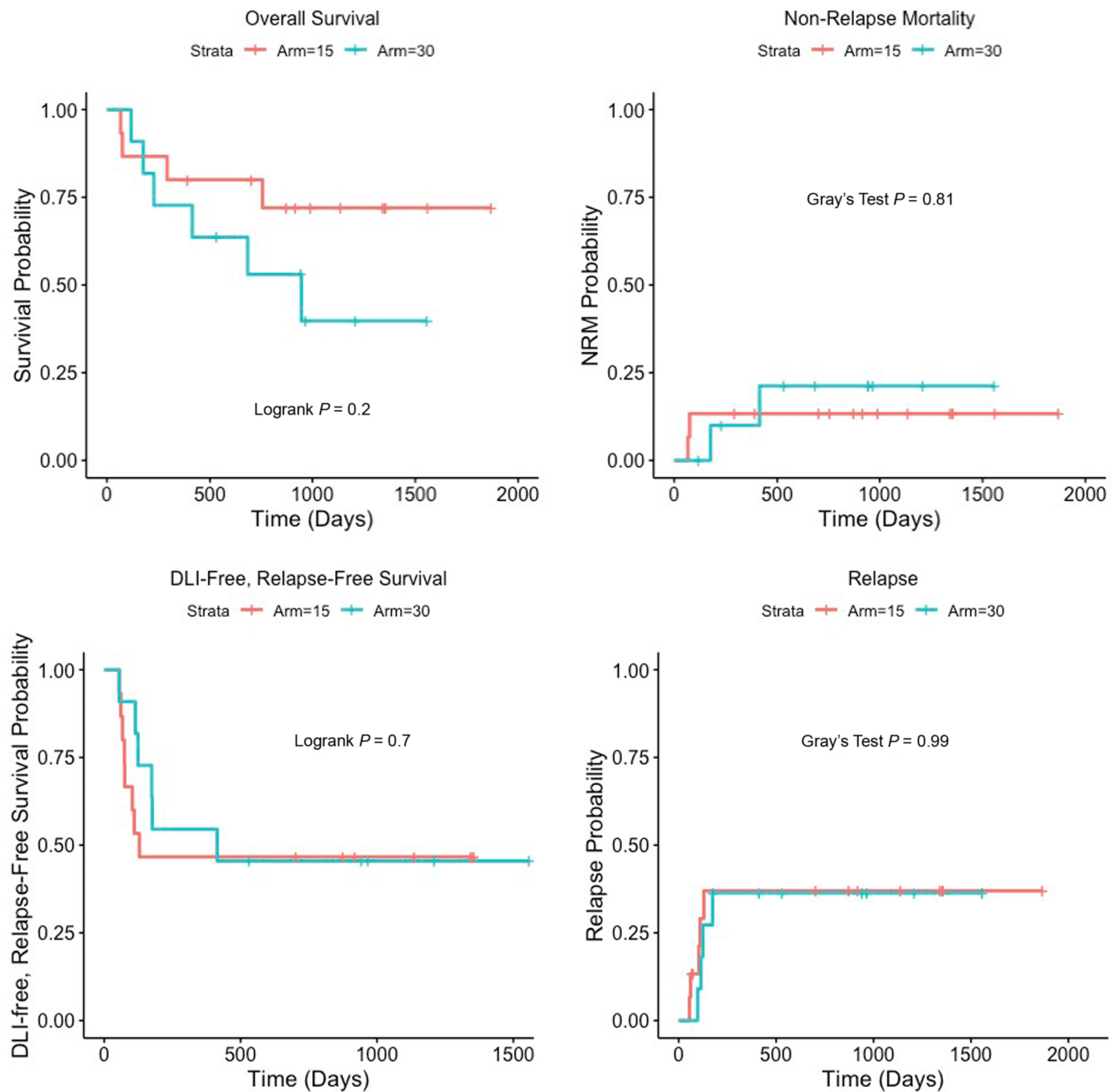
Figure 1. Clinical outcomes following HCT. Relapse and NRM are competing events in the cumulative incidence curves. Log Rank and Gray's test were used for calculating the significance of difference between study arms.

moderate-to-severe cGVHD (HR; 1.018, $P = 0.035$), which corresponds to the observation of patients in the MMF15 arm having both higher CD4 counts and greater tendency to develop cGVHD (Supplementary figure 3). Superior NK-cell recovery on Days 30 and 60 was associated with improved OS (day 30 HR; 0.9906, $P = 0.031$, day 60 HR; 0.9886, $P = 0.016$), paralleling the trend towards improved survival and early superior NK recovery in the MMF15 arm.

T-cell receptor beta (TRB) repertoire evolution

T-cell receptor beta sequencing demonstrated that patients in the MMF15 (+GM-CSF) arm ($N = 10$ at

ddCD3 Recovery Post Transplant
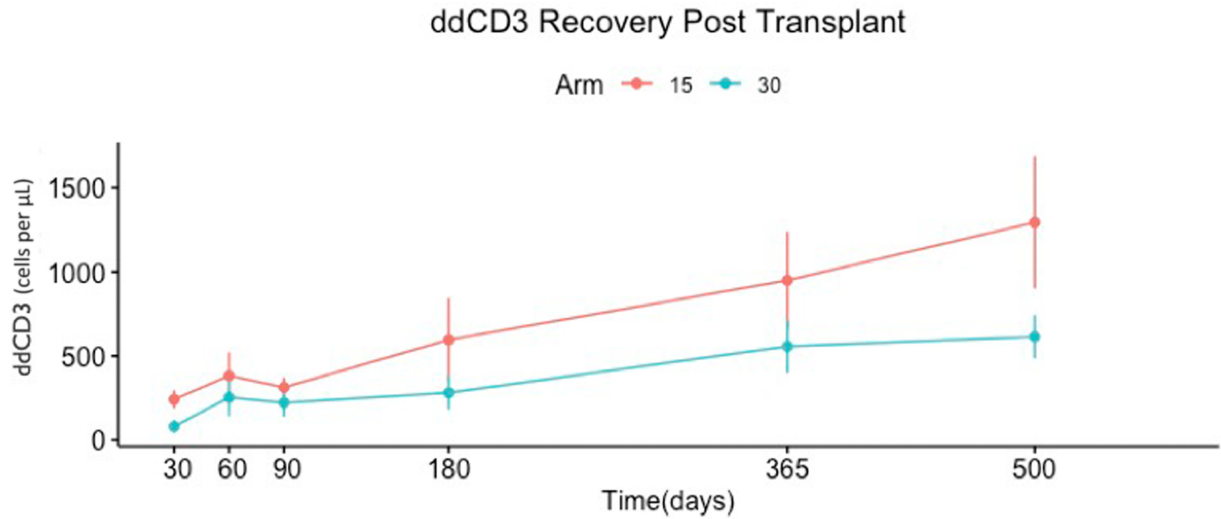
Day	MMF15 ddCD3 N	MMF30 ddCD3 N	MMF15 mean	MMF30 mean	Wilcoxon *P*
30	15	11	241 ± 53.5	81.34 ± 36.8	0.008
60	14	11	383.0 ± 138.9	254.1 ± 110.4	0.338
90	13	11	313.6 ± 56.5	222.2 ± 81.3	0.147
180	13	9	596.7 ± 246.7	281.8 ± 101.4,	0.083
365	11	8	950 ± 288.7	432.4 ± 143.6	0.148
500	10	7	1249.3 ± 392.9	614.6 ± 127.99	0.261

ddCD3 cell Recovery Post Transplant by Donor Type
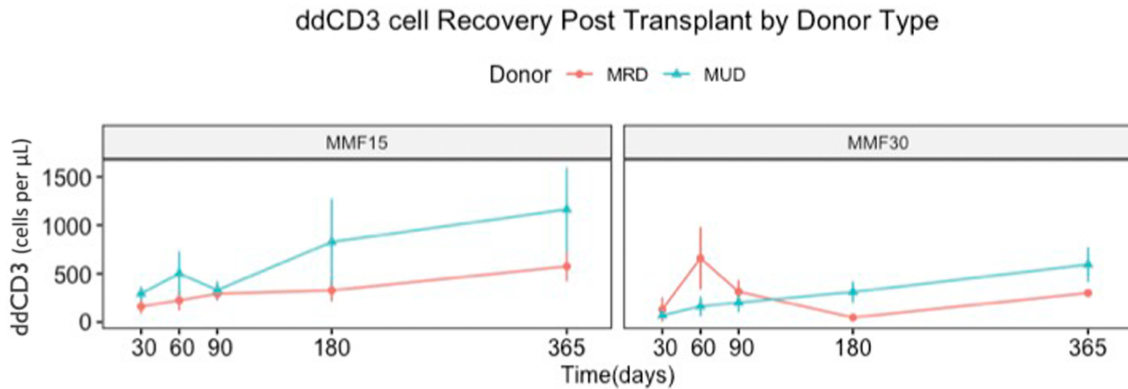
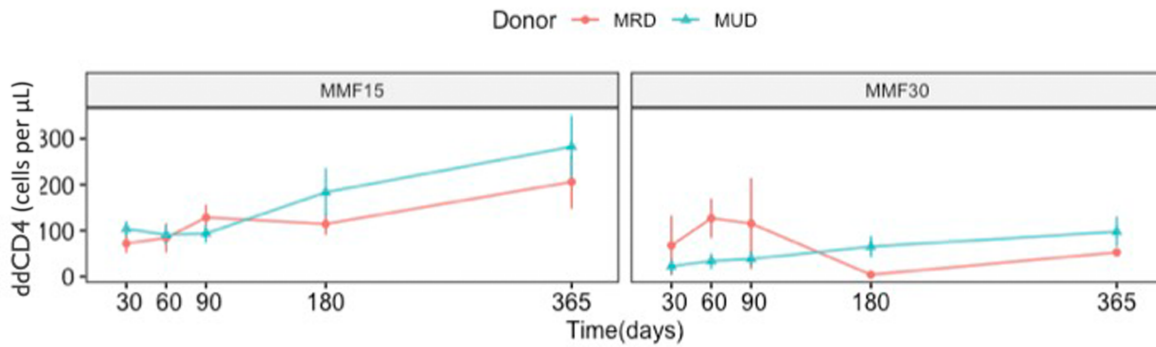| Day	MRD Across Arms	MUD Across Arms	Donor Type Across MMF15	Donor Type Across MMF30
30	1	0.02	0.7	1
60	0.57	0.57	1	0.44
90	1	0.87	1	0.9
180	1	0.72	1	1
365	1	1	1	1

Figure 2. ddCD3 recovery as a function of time post-transplant in MMF15 and MMF30 cohorts, and in MUD and MRD recipients. Values depicted in the figures are listed below the graphs to give *P*-values of paired Wilcoxon tests.

ddCD4 Recovery Post Transplant
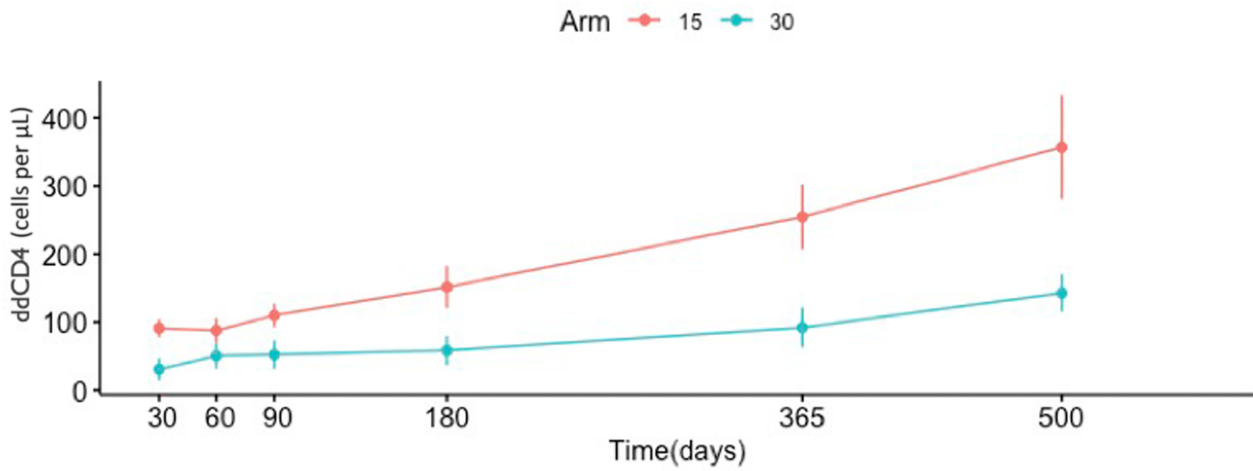
Day	MMF15 ddCD4 N	MMF30 ddCD4 N	MMF15 mean	MMF30 mean	Wilcoxon *P*
30	15	11	91.1 ± 13.2	30.8 ± 16.35	0.002
60	14	11	87.9 ± 18.1	50.7 ± 18.5	0.060
90	13	11	109.8 ± 16.8	52.4 ± 20.6	0.011
180	13	9	151.6 ± 30.84	58.3 ± 21.3	0.009
365	11	8	254.7 ± 47.3	92.0 ± 29.2	0.015
500	10	7	365.9 ± 76.3	142.6 ± 27.2	0.009

ddCD4 cell Recovery Post Transplant by Donor Type

Day	MRD Across Arms	MUD Across Arms	Donor Type Across MMF15	Donor Type Across MMF30
30	1	0.02	1	1
60	1	0.07	1	0.36
90	1	0.08	1	1
180	0.89	0.12	0.89	0.89
365	1	0.1	1	1

Figure 3. ddCD4 recovery as a function of time post-transplant in MMF15 and MMF30 cohorts, and in MUD and MRD recipients. Values depicted in the figures are listed below the graphs to give *P*-values resulting from paired Wilcoxon tests.

ddCD8 Recovery Post Transplant

Arm ● 15 ● 30
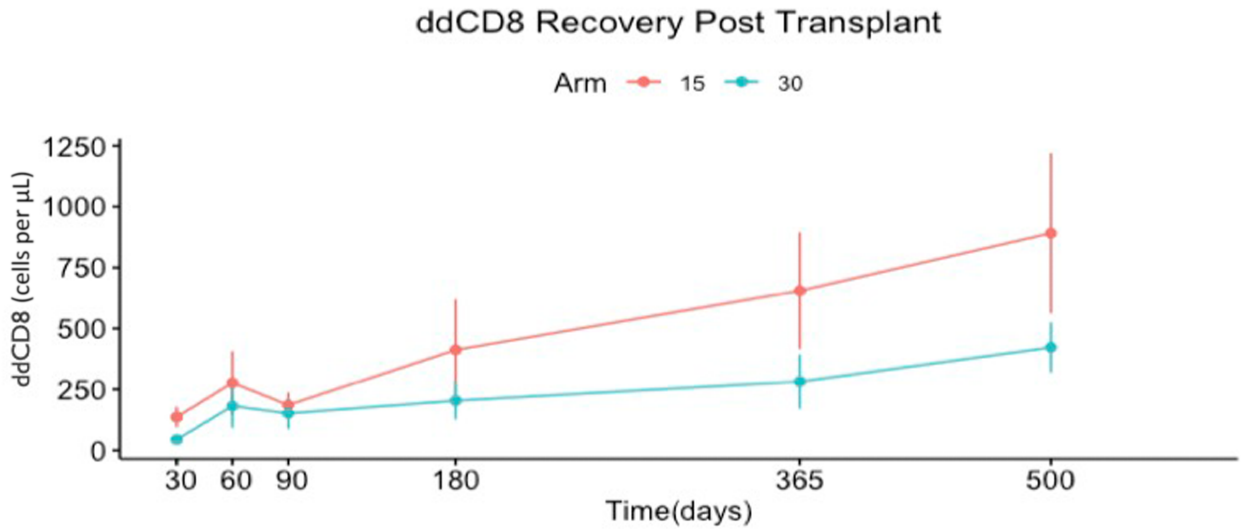
Day	MMF15 ddCD8 N	MMF30 ddCD8 N	MMF15 mean	MMF30 mean	Wilcoxon *P*
30	15	11	136.5 ± 41.5	43.8 ± 19.1	0.029
60	14	11	276.7 ± 129.1	181.8 ± 89.3	0.460
90	13	11	185.7 ± 51.2	151.5 ± 64.2	0.524
180	13	9	412.2 ± 207.63	203.7 ± 76.9	0.350
365	11	8	655.1 ± 238.6	281.9 ± 110.6	0.159
500	10	7	891.4 ± 328.36	433.3 ± 102.5	0.591

ddCD8 cell Recovery Post Transplant by Donor Type

Donor ● MRD ● MUD
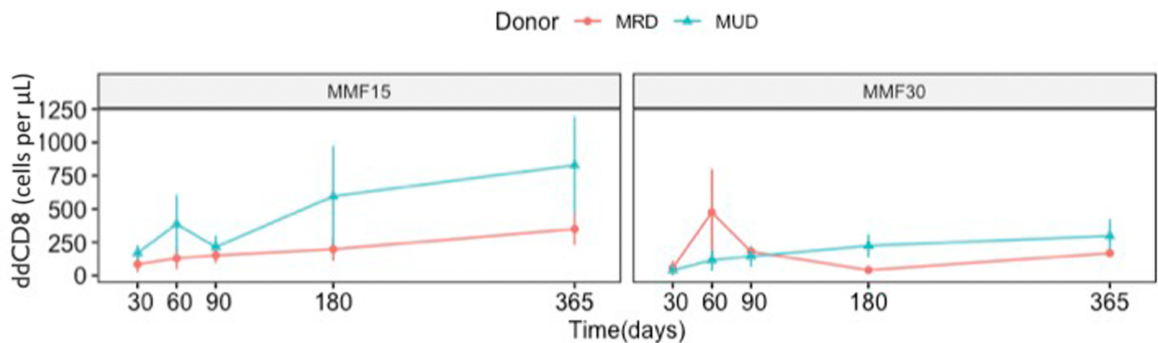
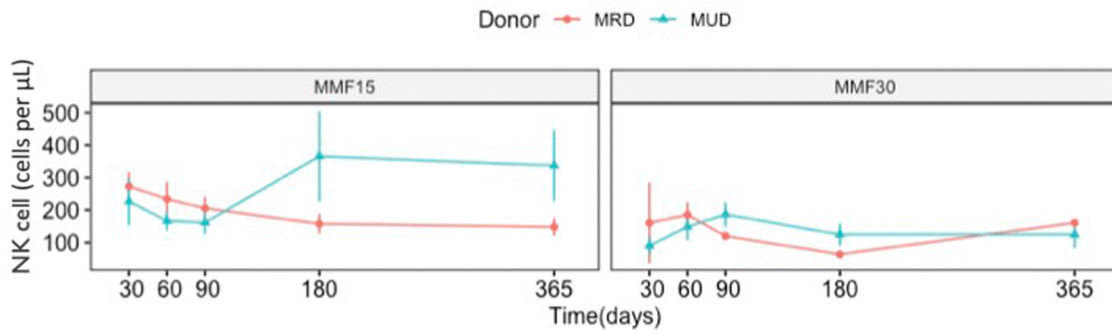| Day	MRD Across Arms	MUD Across Arms	Donor Type Across MMF15	Donor Type Across MMF30
30	1	0.048	0.18	1
60	0.71	0.71	1	0.44
90	1	1	1	1
180	1	1	1	1
365	1	1	1	1

Figure 4. ddCD8 recovery as a function of time post-transplant in MMF15 and MMF30 cohorts, and in MUD and MRD recipients. Values depicted in the figures are listed below the graphs to give *P*-values resulting from paired Wilcoxon tests.

NK cell Recovery Post Transplant
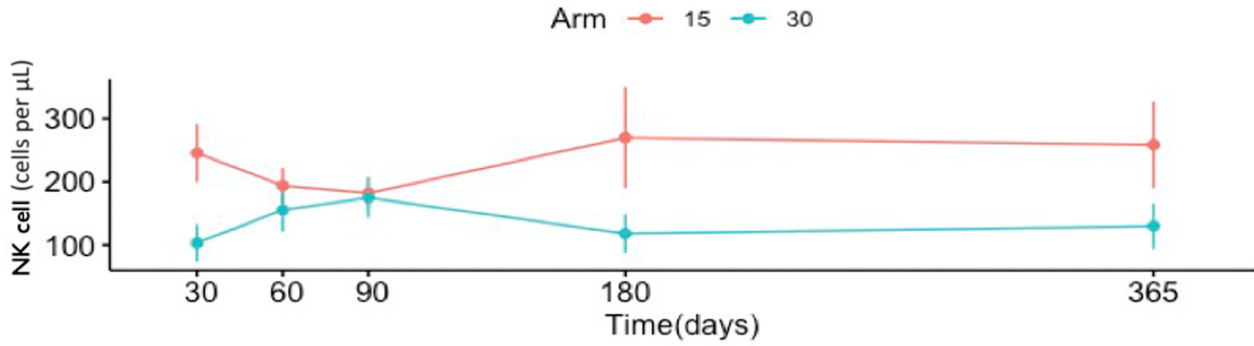
Day	MMF15 CD56 N	MMF30 CD56 N	MMF15 mean	MMF30 mean	Wilcoxon *P*
30	15	11	245.3 ± 45.7	103.2 ± 29.3	0.0239
60	15	11	193.8 ± 27.7	155.6 ± 34.0	0.4361
90	13	11	181.9 ± 24.9	174.5 ± 31.4	0.7280
180	13	9	269.6 ± 79.3	117.8 ± 30.3	0.0353
365	12	7	258.5 ± 68.3	129.8 ± 35.8	0.1630

NK cell Recovery Post Transplant by Donor Type

Day	MRD Across Arms	MUD Across Arms	Donor Type Across MMF15	Donor Type Across MMF30
30	0.86	0.47	0.72	1
60	1	1	1	1
90	1	1	1	1
180	1	0.17	0.69	1
365	1	0.8	1	1

Figure 5. NK-cell recovery as a function of time post-transplant in MMF15 and MMF30 cohorts, and in MUD and MRD recipients. Values depicted in the figures are listed below the graphs to give *P*-values resulting from paired Wilcoxon tests.

CD19 Recovery Post Transplant

Arm ● 15 ● 30
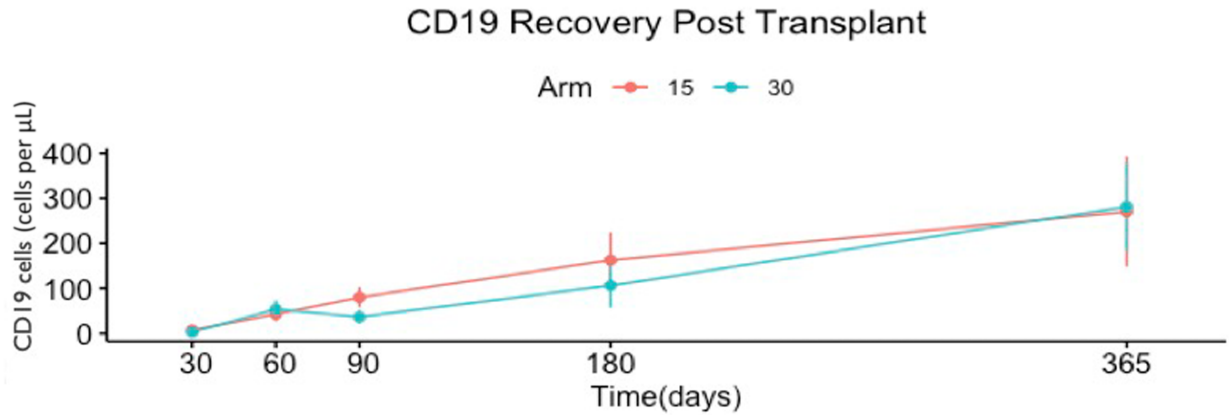
Day	MMF15 CD19 N	MMF30 CD19 N	MMF15 mean	MMF30 mean	Wilcoxon P
30	15	11	7.5 ± 1.6	2.7 ± 0.5	0.0168
60	15	11	42.6 ± 15.2	53.6 ± 19.6	0.8350
90	13	11	80.1 ± 22.1	36.6 ± 14.7	0.0984
180	13	9	162.8 ± 61.7	106.3 ± 48.6	0.5477
365	12	7	270.5 ± 121.9	281.3 ± 97.1	0.2539

CD19 cell Recovery Post Transplant by Donor Type

Donor ● MRD ▲ MUD
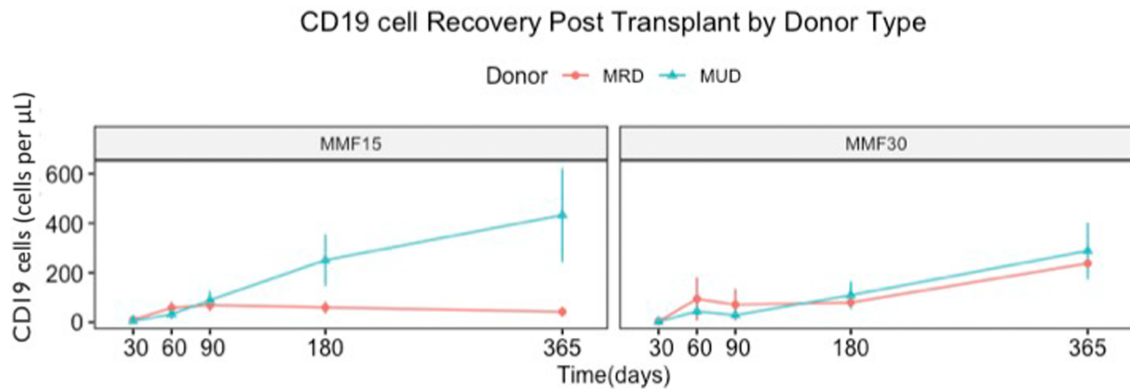
Day	MRD Across Arms	MUD Across Arms	Donor Type Across MMF15	Donor Type Across MMF30
30	0.62	0.62	0.62	1
60	1	1	1	1
90	1	1	1	1
180	1	1	1	1
365	1	1	0.06	1

Figure 6. B-cell recovery as a function of time post-transplant in MMF15 and MMF30 cohorts, and in MUD and MRD recipients. Values depicted in the figures are listed below the graphs to give P-values resulting from paired Wilcoxon tests.
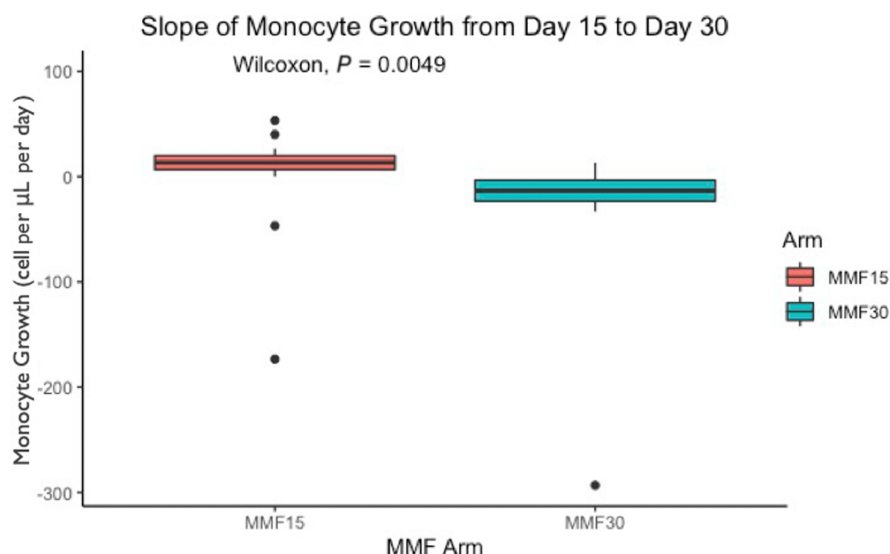
Figure 7. Change in monocyte count between Day 15 and Day 30 between MMF15 and MMF30 groups.

Day 30; 9 at Day 100) compared with those in the MMF30 arm ($N = 9$ at Day 30; 10 at Day 100), consistently had a trend towards a greater number of unique productive TRB gene rearrangements, (median 26 686 vs. 12 892 at Day 30; 31 324 vs. 15 345 at Day 100, P = NS), and productive templates (56 785 vs. 22 528 at Day 30; 65 458 vs. 32 082 at Day 100 P = NS). This finding was consistent with the observed greater $CD3^+$ T-cell count recovery recorded at these time points in the MMF15 cohort. Simpson's clonality calculated for productive TRB sequences was also lower for the MMF15 arm at Day 100 (0.07 vs. 0.06 at Day 30; 0.07 vs. 0.12 at Day 100 P = NS) indicating the evolution of a potentially more diverse T-cell repertoire in this study arm (Figure 8). The T-cell repertoire was then analysed on an individual level with the 10 highest frequency T-cell clones at Days 30 and 100 being identified and tracked. An obvious change in clonal hierarchy was observed in most patients, with low-frequency T-cell clones at Day 30 growing to become dominant by Day 100 and *vice versa*. There was no obvious difference between the study arms with respect to the change in the dominant clones (Supplementary figure 4).

Productive TRB gene rearrangements and templates were plotted against simultaneously measured absolute $CD3^+$ T-cell counts in circulation, adjusted for volume of blood sequenced, to give an integrated representation of the T-cell repertoire recovery in individual patients, at each time point. On average, patients in the MMF15 (+GM-CSF) arm had values distributed farther from the *origin* in this two-dimensional 'T-cell recovery plane' integrating the T-cell receptor beta repertoire with T-cell count in circulation (Figure 9a). In this hypothetical plane, distance from the *origin* is proportional to the size and clonal diversity of the T-cell population. When the changes in these values in individual patients were mapped across the T-cell recovery plane from Day 30 to Day 100, it was largely observed along the *x*-axis (T-cell counts) in most patients, because of a relatively larger increase in T-cell counts as opposed to number of rearrangements (Figure 9b). This indicated that the T-cell clonal emergence is most active during the first few weeks after HCT, with growth of individual clones occurring subsequently over time. This supports the importance of early-term immune recovery during the transplant process in defining clonal diversity that emerges during that period. Even though these data are available for a small number of patients, there was a suggestion of improved outcomes in patients where the T-cell repertoire was farther from the origin (Figure 10).

DISCUSSION

In this study, recipients of allogeneic HCT underwent a uniform immunoablative conditioning regimen with rabbit ATG and reduced intensity TBI.
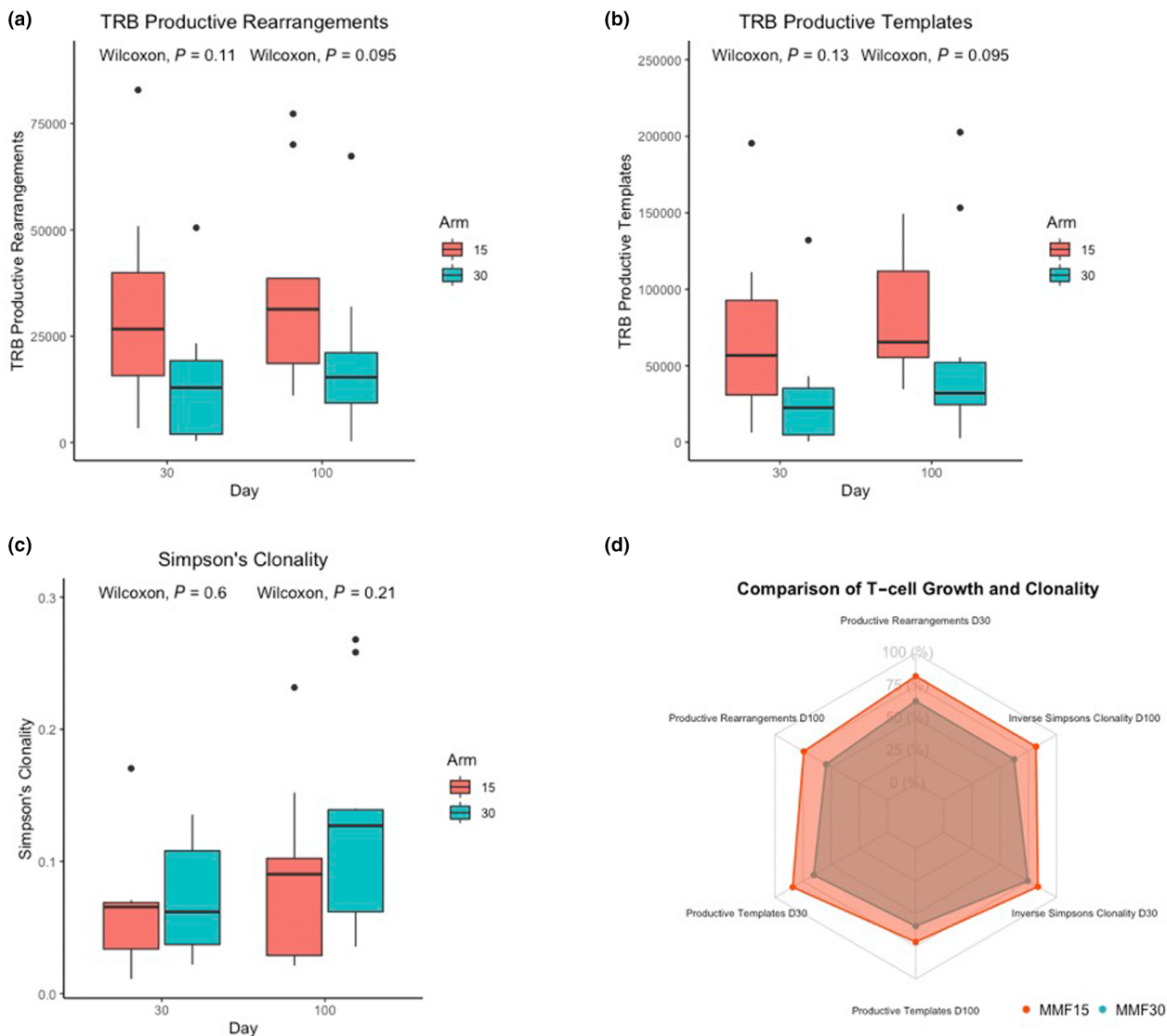
Figure 8. T-cell receptor beta repertoire assessed by next-generation sequencing. **(a)** TRB rearrangements, **(b)** TRB templates and **(c)** Simpson's clonality for MMF15 and MMF30 patients. Plot **(d)** depicts a summary of the differences in TCR diversity between Days 30 and 100. Inverse Simpsons Clonality Index is utilised for consistency in visualisation of higher values referring to greater magnitude of the measured variable. As each variable has its own scale, the *y*-axis of each vertex ranged from their respective minimum to maximum within the dataset.

The duration of intense post-transplant immune suppression was varied in the two study arms, as were the cytokines given for promoting engraftment. Patients who received a shorter course of intense immune suppression and GM-CSF had more rapid and sustained T-cell recovery with the trend continuing for the first year following transplant. The T-cell repertoire emerging post-transplant was also more diverse in this group. Differences in donor-derived immune recovery were associated with clinical outcome differences in the two study arms. There was a greater likelihood of acute GVHD in those with rapid cytotoxic T-cell recovery in the first month following transplant, and more chronic GVHD in those with more rapid helper T-cell recovery. Consistent with these T-cell recovery patterns there was a trend for improved survival and more moderate-to-severe chronic GVHD in the patients treated with short course MMF and GM-CSF. These findings imply that small early differences in immune suppression such as, reduction in the duration of intense immune
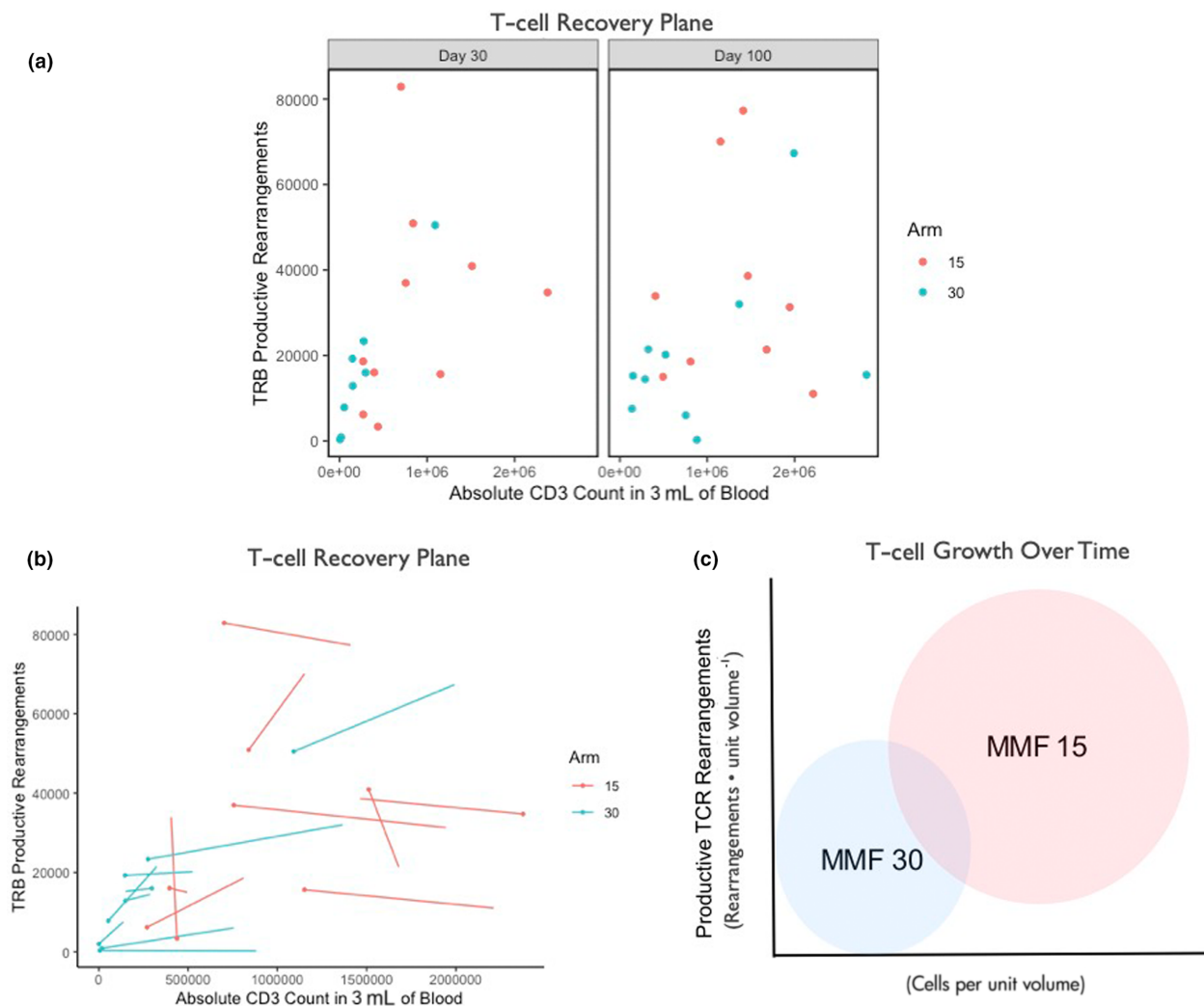
Figure 9. (a) T-cell repertoire characteristics plotted in the two-dimensional 'T-cell recovery plane', showing T-cell number (abscissa) and corresponding TRB rearrangements (ordinate) at Days 30 and 100 from the MMF15 (red) and 30 cohorts (blue). **(b)** T-cell repertoire evolution plotted in individual patients over time from Day 30 to Day 100 ($N = 9$ paired observations for each cohort. MMF15, Red; MMF30, Blue). **(c)** Model depicting distribution of the T-cell repertoire in the two cohorts within the T-cell recovery phase space.

suppression and potentially augmented antigen presentation, may lead to long-term differences in immune reconstitution. Our study cohort is small, but the findings reported support the notion that post-transplant immune recovery and clinical outcomes following HCT are not entirely probabilistic, but may be impacted in a predictable manner by early adjustments to immune modulation. Adjustments to immunosuppressive therapy should thus be studied as a function of time following different GVHD prophylaxis regimens with real-time monitoring of T-cell recovery over time and its influence on clinical outcomes.

Before expanding on the findings from this study, it is important to outline its shortcomings. The trial was originally designed to investigate differences in 1-year, DLI-free and relapse-free survival between the study and control arms of the trial. The study accrual goal could not be met because of declining trial referral. In a single institution setting, this was likely related to contemporary advances in the pharmacotherapy of relapsed lymphoma and myeloma, as well as the availability of chimeric antigen receptor T-cells, which reduced the desirability of allografting for these conditions. Improvements in supportive care protocols with myeloablative conditioning (MAC)
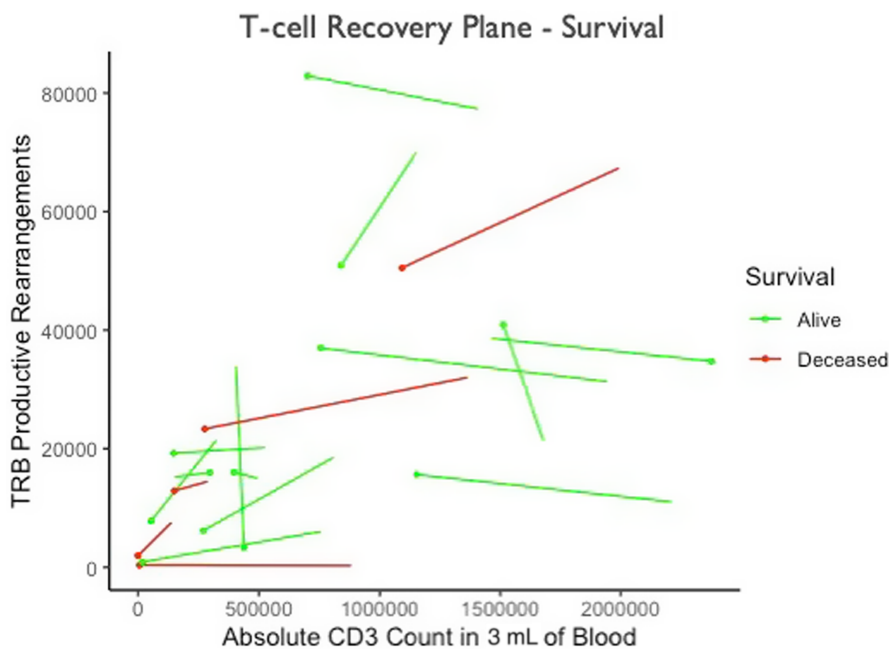
Figure 10. (a) Different probability distribution of survival in different regions of the T-cell recovery plane, probability of survival 0.86 vs. 0.64 ($P = 0.56$, Fisher's exact test) in the area beyond the region closer to the origin, bounded by values, 10^6 T-cells (*x*-axis) & $3 * 10^4$ (TCR rearrangements on the *y*-axis) describing the T-cell repertoire.

regimens further reduced study referrals for myeloid disorders using this immunoablative approach. As a consequence, aside from the usual single-centre transplant trial issues around heterogeneity of donor and disease states, this trial is burdened with low numbers. Thus, the conclusions from this study must be interpreted keeping in mind its limitations, particularly with respect to clinical outcomes reported. Nevertheless, because of adaptive randomisation, the specific nature of the surrogate end point chosen (immune reconstitution at 8 weeks) and the immune reconstitution data collected and analysed, the authors posit that the T-cell recovery data are robust and extrapolatable to future similar endeavours.

The results reported here highlight two aspects of transplant immunobiology: first, its evolving nature as a function of time, and second, the crucial impact of the very first few days following transplant. This underscores the differential effect of immune suppression in the early-term following transplantation and its long-term impact. Similar effects have been observed with low-dose methotrexate given for GVHD prophylaxis, where omission of the fourth dose was associated with better survival and lower relapse rate in recipients of marrow allografts.[39]

There is a substantial body of literature where ATG given with pharmacokinetic guidance yields improved outcomes in umbilical cord blood recipients,[25,40] and those with optimal ATG levels and unrelated donor transplantation have improved survival.[41] Suboptimal levels resulted in higher risk of nonrelapse mortality and supra-optimal levels in relapse related mortality among these patients. Therefore, varying impact of immune suppression intensity during the first few days to weeks following transplantation needs to be considered for optimising outcomes.

The findings reported here demonstrate the principle that immune recovery may be *modulated* with interventions in the immediate aftermath of HCT. A reduction in the duration of intense immune suppression, combined with GM-CSF administered to potentially augment antigen presenting function in this instance increases the rate of T-cell recovery in patients thus treated. Risk of acute or chronic GVHD is increased with different T-cell subsets recovering over time and may impact survival. As the change in therapy reported here elicits an immune response, ongoing therapeutic adaptation to the evolving T-cell milieu with treatment interventions may mitigate adverse events in the long term. As an example, patients

with an elevated CD8^{+} T-cell count early on may benefit from an intensification of the calcineurin inhibitor therapy or introduction of additional GVHD prophylactic measures such as abatacept therapy, extra-corporeal photopheresis, anti-interleukin 6 antibodies or CD28 blockade. Patients with an elevated CD4^{+} count may need to continue their calcineurin inhibitor for a longer period than the conventional 6 months post-transplant. The larger point to be made here is that ongoing surveillance of immune recovery and real-time adjustment of immune suppression on an ongoing basis for many months after transplantation is imperative for reducing the risk of toxicities following HCT.

The second takeaway message from these trial results is the influence that early intervention has on longer term outcomes. In this instance, the MMF given over the first 15 days after HCT yielded comparable control of GVHD as the longer regimen, with improved immune recovery after discontinuing this agent. Time and again very early intervention following HCT, such as administration of post-transplant cyclophosphamide in haploidentical transplants, has demonstrated an enduring impact which lasts long into the course of transplant.[42] The shorter course of MMF was chosen in this instance to mimic the time course of post-transplant methotrexate, which is administered for a short period, but has a significant influence on the longer term course. In this study, early discontinuation of MMF following engraftment allowed for optimal NK and T-cell recovery, without a significant increase in risk of severe GVHD and with reliable engraftment.

Granulocyte-macrophage colony stimulating factor was utilised in this study to augment monocyte differentiation into antigen presenting dendritic cells, and while numerically, there was no difference in the magnitude of monocyte recovery between the two arms, it is expected that this cytokine would have contributed to the phenotypic maturation of antigen presenting cells[43] and to potentially greater T-cell subset numeric recovery and clonal diversity observed.[44,45] Recently, GCSF has been implicated in augmenting ATG mediated clearance of T-cells in patients with a higher level of ATG in circulation at the time of neutrophil engraftment.[46] This was associated with worsening TRM and survival following allografting.[47] This mechanism may have potentially contributed to the better T-cell recovery observed in the MMF15 arm because of slower neutrophil

recovery with GMCSF. Early T-cell and T-cell subset recovery was observed in patients with sustained monocyte recovery from Day 15 to Day 30 post-transplant, which was more commonly seen in the MMF15 arm, likely because of a combination of short course MMF and GMCSF. While these innate-adaptive immune homeostatic influences may contribute to T-cell growth, augmented antigen presentation and antigen-driven T-cell expansion may also have contributed to the immune recovery observed.

To investigate the potential role of greater antigen-driven T-cell expansion, the T-cell receptor beta repertoire was studied using next-generation sequencing (NGS). Over the last decade, TRB repertoire reconstitution as measured by NGS has emerged as a robust measure of T-cell recovery. These large data sets are reported using a variety of diversity indices, such as Simpson's Clonality Index and Shannon's entropy. T-cell clones have two unique aspects that impact their function, their ability to identify antigens through VDJ recombined T-cell receptors and the frequency of these unique TCR bearing T-cell clones. These two properties of bulk reconstitution of T-cell populations post-transplant were modelled in a hypothetical 'T-cell recovery plane', and demonstrated that patients in the MMF15 arm had a more numerous and diverse T-cell repertoire than those in the MMF30 arm. Importantly, this T-cell recovery modelling demonstrated that the period of development of greatest T-cell clonal richness is the first month following transplant. Subsequent to that, the dominant effect is numeric expansion of T-cells, with comparatively smaller change in the overall number of T-cell clones. Looking beyond the large-scale T-cell repertoire growth in patients, when individual T-cell clones are followed over time, considerable variability in terms of clonal growth dynamics is observed with change in hierarchy. Low-frequency clones in the early post-transplant period grow to become dominant in most patients. These changes occur in the context of the large-scale T-cell recovery, and suggest an antigen-driven proliferation mechanism as opposed to simple homeostatic T-cell expansion following transplant. Larger cohorts will allow distinction between oligoclonal expansions and different clinical states, within the context of large-scale T-cell population recovery.

Nonmyeloablative and RIC HCT is complicated by high rates of GVHD.[48] T-cell depletion with

ATG reduces the risk of chronic GVHD in RIC HCT[49]; however, if infections, recurrent disease and autologous reconstitution are to be minimised,[50] optimising postengraftment immune suppression is critical. The original MMF-containing regimens were critical in preventing both GVHD and graft rejection, and while the former is mitigated with ATG, the autologous T-cell recovery may be seen late after transplant when ATG is used. Reducing intense immune suppression in the early days following transplantation would counter this by improving early donor T-cell recovery. Reduction in the duration of myelosuppression from MMF with administration of GM-CSF likely has a synergistic effect of the innate-adaptive immune interaction, as in the monocyte-T-cell interactions. These effects will require more detailed molecular and immunophenotypic characterisation in future studies, to understand difference in the engraftment kinetics of different T-cell and monocyte-/dendritic- cell subsets in patients getting GCSF vs. GM-CSF. Sustained myeloid recovery and consequent T-cell reconstitution were likely related to the duration of MMF and the cytokine utilised in the study arm, as well as the dendritic-cell differentiation of monocytes.

In conclusion, the risk of compromised immune recovery, with respect to both magnitude and diversity, in recipients of ATG in RIC HCT may be overcome by reducing the duration of intense immune suppression post-transplant and by utilising GM-CSF. Patients with immune recovery have improved outcomes, evident even in a small, heterogeneous cohort of HCT recipients. Constant measurement of immune reconstitution and adjustment of immune suppression following HCT is a necessary condition for optimising clinical outcomes. The small size of this study cohort limits the clinical applicability of these findings; however, they provide a quantitative insight into the pathophysiology of T-cell recovery post-transplant and may serve to inform future trial design.

METHODS

Patients and adaptive randomisation scheme

The reported study was an adaptively randomised, phase 2, open-label, trial (NCT02593123), approved by the Virginia Commonwealth University IRB (MCC-14-10 739). Inclusion criteria included high risk or recurrent hematologic malignancy, and availability of 8/8 or 7/8, high-resolution HLA-A, -B, -C, and DRB1-matched, related (MRD) or unrelated donor (MUD). Allocations to the study and control arms was stratified based on (1) lymphoid versus myeloid malignancy and (2) donor type, MRD vs. MUD (Table 1). The primary end point to be examined in this study was difference in DLI-free/relapse-free survival between the investigational and control arms, with secondary end points being survival, graft vs. host disease, DLI use and T-cell recovery. Expected total recruitment and number used for statistical power analysis was 60 patients to demonstrate a 15% improvement in DLI-free/relapse-free survival at 1 year. An adaptive randomisation scheme was utilised to increase the probability of optimal patient outcomes,[51] with the hypothesis that patients in the MMF15 arm will have superior donor-derived T-cell recovery at 8-week post-transplant, with superior DLI-free and relapse-free survival in these patients. The stratification algorithm was a doubly adaptive biased coin design (DBCD) coupled with optimal allocation of continuous outcome[52]; in this case, the donor-derived CD3^{+} (ddCD3) T-cell count at 8-week post-transplant was utilised. This was calculated by the following formula: $ddCD3 = absolute\ CD3^+\ cell\ count * fraction\ donor\ chimerism\ in\ T\text{-}cells$. This surrogate marker was chosen because a higher ddCD3 count on Day 60 was previously shown to be associated with improved outcomes in an earlier cohort of the ATG-TBI conditioned patients with GVHD prophylaxis as delivered in the control arm.[38] A two-patient lead-in was used, with the initial enrollment in MMF30:MMF15 arms being 1:1. As the first two patients reached the 8-week milestone and their ddCD30 data were collected, the randomisation of later trial participants favored the trial arm that resulted in a higher average ddCD3 on D60. This average was recalculated on a rolling basis. Details regarding adaptive randomisation and study stopping criteria are provided in methods in the Supporting information file.

Conditioning and study schema

All patients were conditioned with rabbit ATG (Thymoglobulin, Sanofi-Aventis, Bridgewater, NJ, USA) given at a dose of 1.7 mg kg^{-1} per day from Day −9 through to Day −7 (total dose 5.1 mg kg^{-1}), and 1.5 Gy total body irradiation (TBI) administered twice daily on Day −1 and once on Day 0 for a total dose of 450 cGy given in three fractions.[24,25] Patients randomised to the investigational cohort (MMF15) received mycophenolate mofetil (MMF) dosed at 15 mg kg^{-1} every 12 h from Day 0 to Day 15 and administered subcutaneous granulocyte-macrophage colony stimulating factor (GM-CSF) (Sargramostim, Partner Therapeutics, Lexington, MA, USA) 250 μg m$^{2\ -1}$ per day from Day 4 until haematopoietic reconstitution; those on the control arm (MMF30) received MMF dosed at 15 mg kg^{-1} every 12 h from Day 0 to Day 30 and received subcutaneous granulocyte colony stimulating factor (G-CSF) (Filgrastim, Amgen, Thousand Oaks, CA, USA) 5 μg kg^{-1} per day from Day 4 through haematopoietic reconstitution. GVHD prophylaxis consisted of tacrolimus from Day −2 through to Day 90 followed by a 2–3-month-long tapering schedule. In the first month, tacrolimus levels were maintained in a 10–15 ng mL^{-1} range, dropping down to 8–12 ng mL^{-1} in the next 2 months generally. Patients in the

investigational cohort were also given inhaled fluticasone twice daily from Day 4 until discontinuation of GM-CSF to minimise pneumonitis risk.

Engraftment and immune reconstitution

Circulating absolute monocyte, lymphocyte (ALC) and neutrophil count (ANC) were determined as a part of routine complete blood counts using a haematology analyser (XN-9000; Sysmex, Lincolnshire, IL, USA). $CD3^+$, $CD3^+/CD4^+$, $CD3^+/CD8^+$, $CD19^+$ and $CD56^+/16^+$ cells were measured on days 30, 60, 90, 180, 365, and 500 using a FACSCanto II flow cytometer (BD Biosciences, San Jose, CA, USA). Donor T-cell chimerism was also measured at these time points using PCR for short tandem repeats on DNA isolated from T-cells isolated using anti-$CD3^+$ immunomagnetic beads. Donor-derived T-cell and T-cell subset counts (ddCD3, ddCD4 and ddCD8) were determined by calculating the product of the following: *absolute subset cell count * fraction donor chimerism in T-cells*. The relationship between early monocyte (Day 15 and Day 30) and T-cell recovery (Day 30) was studied using the least absolute shrinkage and selection operator (LASSO) to help smooth outcome values over the Day 15 and Day 30 monocyte count plane; the area of the two-dimensional window was selected by grid search through potential side lengths (50–500, by 50), selecting those that lead to largest adjusted R^2 in a two-factor regression with interaction. From this optimal window, the smoothed counts for ddCD3, ddCD4 and ddCD8 were (separately) modelled against fixed effects of Day 15 monocyte counts, Day 30 monocyte counts and their interaction. Interaction plots were constructed to show estimated associations between monocyte counts on Day 15 and Day 30, and ddCD3, ddCD4 or ddCD8 cell counts, and adjusted at the 25th and 75th percentiles of the second monocyte measure, either Day 30 or Day 15, respectively. Sustained monocyte recovery between the two study arms was determined by calculating the gradient, $\nabla_{Mo} = \frac{\Delta Mo_{30-15}}{\Delta t}$, where ΔMo_{30-15} is the difference in monocyte count in a patient between Days 15 and 30, and Δt is 15 days. RStudio was used for all data management and modelling.

T-cell receptor beta sequencing

T-cell receptor beta sequencing was performed using genomic DNA from the transplant recipients, obtained on approximately Days 30 and 100, using the Adaptive Biotechnologies® immunoSEQ® human T-cell receptor beta (hsTCRB) Kit (Adaptive Biotechnologies, Seattle, WA, USA). Genomic DNA was isolated from cryopreserved cell pellets obtained by processing 3 mL of blood, using DNeasy Blood & Tissue Kit and concentrated using Zymo Research DNeasy Blood & Tissue Kit following the manufacturer's instructions. DNA concentration was determined using Promega QuantiFluor dsDNA System kit and DNA integrity was determined by electrophoresis in an 0.8% agarose gel. Four genomic DNA replicates per sample, each containing on average approximately 4.0 μg were independently amplified using Qiagen 2× Multiplex PCR Master mix with proprietary immunoSEQ® hsTCRB primers. The amplicons were diluted (1:4) and submitted to a second round of PCR amplification to add sample-specific barcodes and Illumina adapters to each PCR replicate. The final amplicons were combined into two

pools (containing 23 and 17 DNA samples, respectively) and cleaned up with magnetic beads provided in the kit. Pools were purified on the Sage Science BluePippin DNA size selection system to remove primer dimers and other contaminating amplicons. A BluePippin 2% dye-free agarose gel cassette was used to capture DNA in a target range of 240–400 base pairs. After completion of size selection, ∼ 50 μL of size selected libraries were removed from the elution wells, cleaned and concentrated using 1.8× Agencourt AMPure XP magnetic beads. Cleaned-size selected DNA libraries were eluted in 28 μL of Takara DNA suspension buffer. Size selection was assessed using an Agilent Bioanalyzer using a High-Sensitivity DNA Chip. Final DNA libraries were quantified using the KAPA Library Quantification Kit. Sample pools were denatured with 0.2 N NaOH, diluted into Illumina Hybridization Buffer to 10 pM and combined with 5% PhiX control sequences, following the standard Illumina guidelines. Samples were sequenced on the Illumina MiSeq instrument using MiSeq Reagent Kit v3 (150-cycle). The raw sequencing data were uploaded to Adaptive Biotechnologies immunoSEQ® ANALYZER and processed using the company's proprietary analysis pipeline. Results for each DNA sample were reported after merging data from the four replicates of each sample. Unique T-cell receptor beta (TRB) gene rearrangements and templates in these samples were quantified and Simpson's clonality determined (ImmunoSeq Analyzer 3.0).[53] The *Track Rearrangements* function within the ImmunoSEQ ANALYZER software was used to track the top 10 clones on days 30 and 100. This allowed for visualisation of the clonal hierarchy within the TCR repertoire over time within individual patients.

T-cell repertoire recovery analysis

Conventional immune reconstitution studies look at T-cell recovery and TRB sequencing information as distinct entities; however, these are two aspects of the same entity: the T-cell repertoire, which evolves over time following HCT. The $CD3^+$ cell count measures the number of circulating T-cells, while the TRB sequencing measures the clonal makeup of the circulating T-cells, each clone identified by its unique T-cell receptor (TCR) beta variable, diversity and joining segment recombined sequence. Furthermore, each individual's T-cell repertoire may be modelled in an immune phase space, plotting their T-cell counts against measures of T-cell clonal diversity.[12,15] This representation simultaneously accounts for both the quantitative (T-cell count) and qualitative (TRB clonality) aspects of the T-cell repertoire at any given point in time. T-cell repertoire was plotted in the immune phase space, termed T-cell recovery plane, at Days 30 and 100 for each patient utilising the absolute $CD3^+$ cell count (μL^{-1}) * 1000 to get $CD3^+$ cell counts mL^{-1}. Adjusted for 3 mL, this gave the potential number of T-cells in the sample that the genomic DNA was extracted from. T-cell counts were plotted against the number of productive TRB gene rearrangements present at each time point as a measure of T-cell repertoire recovery.

Statistical analysis

Cell count differences between the two study arms were assessed with the Wilcoxon rank sum test. Clinical outcomes were analysed using Cox proportional hazards with a

univariate model only including the treatment arm (MMF15 vs. MMF30). Multivariate models of the primary outcomes; progression-free survival (PFS), relapse and donor lymphocyte infusion (DLI)-free relapse-free survival outcome analyses were adjusted for treatment arm, donor type and disease (myeloid vs. lymphoid malignancy). Variables, treatment arm, donor type (MRD vs. MUD) and recipient age were applied to OS, NRM and all forms of GVHD. In all Cox proportional hazards analyses involving GVHD, patients were censored at the date of relapse (competing risk) or their first DLI. Cumulative incidence of relapse was similarly censored at the time of NRM and DLI. Cumulative incidence analysis was used to compare both moderate–severe and severe cGVHD, with relapse as a competing event. Gray's test was used to determine significance of differences observed between the two arms. GVHD was graded based on the National Institutes of Health consensus criteria.

The impact of various immune cell populations on clinical outcomes was analysed with Cox proportional hazards analyses. Because of the small study size, all patients were pooled for this analysis, and the study arm was used in the multivariate analysis to account for this variable's effects. Cell counts were considered as continuous variables. Multivariate models including immune cell populations, included trial arm and donor status (MRD vs MUD), with the exception of relapse, and DLI-free and relapse-free survival which included trial arm and myeloid vs lymphoid disease distinction to parallel the other Cox analyses in this study.

ACKNOWLEDGMENTS

AUTHOR CONTRIBUTIONS

Viktoriya Zelikson: Data curation; formal analysis; writing – original draft; writing – review and editing. **Roy Sabo:** Conceptualization; data curation; formal analysis; investigation; methodology; writing – original draft; writing – review and editing. **Myrna Serrano:** Investigation; methodology; writing – original draft. **Younus Aqeel:** Data curation; investigation. **Savannah Ward:** Data curation; investigation. **Taha Al Juhaishi:** Data curation; investigation. **May Aziz:** Investigation; project administration; writing – review and editing. **Elizabeth Krieger:** Investigation; writing – review and editing. **Gary Simmons:** Investigation; writing – review and editing. **Catherine Roberts:** Data curation; funding acquisition; investigation; methodology; project administration; resources; supervision; writing – review and editing. **Jason Reed:** Validation; writing – review and editing. **Gregory Buck:** Investigation; methodology; writing – review and editing. **Amir Toor:** Conceptualization; data curation; formal analysis; funding acquisition; investigation; methodology; project administration; supervision; writing – original draft; writing – review and editing.

CONFLICT OF INTEREST

The authors declare no conflict of interest.

DATA AVAILABILITY STATEMENT

The data that support the findings of this study are available from the corresponding author upon reasonable request.

REFERENCES

1. Della Porta MG, Jackson CH, Alessandrino EP *et al*. Decision analysis of allogeneic hematopoietic stem cell transplantation for patients with myelodysplastic syndrome stratified according to the revised International Prognostic Scoring System. *Leukemia* 2017; **31**: 2449–2457.

2. Scott BL, Pasquini MC, Fei M *et al*. Myeloablative versus reduced-intensity conditioning for hematopoietic cell transplantation in acute Myelogenous leukemia and myelodysplastic syndromes-long-term follow-up of the BMT CTN 0901 clinical trial. *Transpl Cell Ther* 2021; **27**: 483.e1–483.e6.

3. Anasetti C, Logan BR, Lee SJ *et al*. Peripheral-blood stem cells versus bone marrow from unrelated donors. *N Engl J Med* 2012; **367**: 1487–1496.

4. Tsirigotis P, Byrne M, Schmid C *et al*. Relapse of AML after hematopoietic stem cell transplantation: methods of monitoring and preventive strategies. A review from the ALWP of the EBMT. *Bon Mar Transpl* 2016; **51**: 1431–1438.

5. Bacigalupo A. HLA still matters in allogeneic transplants. *Blood* 2021; **138**: 209–211.

6. Goldberg JD, Zheng J, Ratan R *et al*. Early recovery of T-cell function predicts improved survival after T-cell depleted allogeneic transplant. *Leuk Lymph* 2017; **58**: 1859–1871.

7. Horowitz MM, Gale RP, Sondel PM *et al*. Graft-versus-leukemia reactions after bone marrow transplantation. *Blood* 1990; **75**: 555–562.

8. Cullis JO, Jiang YZ, Schwarer AP, Hughes TP, Barrett AJ, Goldman JM. Donor leukocyte infusions for chronic myeloid leukemia in relapse after allogeneic bone marrow transplantation. *Blood* 1992; **79**: 1379–1381.

9. McSweeney PA, Niederwieser D, Shizuru JA *et al*. Hematopoietic cell transplantation in older patients with hematologic malignancies: replacing high-dose cytotoxic therapy with graft-versus-tumor effects. *Blood* 2001; **97**: 3390–3400.

10. Toor AA, Sabo RT, Roberts CH *et al*. Dynamical system modeling of immune reconstitution after allogeneic stem cell transplantation identifies patients at risk for adverse outcomes. *Biol Bl Mar Transpl* 2015; **21**: 1237–1245.

11. Zelikson V, Simmons G, Raman N *et al*. Dynamical systems modeling of early-term immune reconstitution with different antithymocyte globulin administration schedules in allogeneic stem cell transplantation. *Transpl Cell Ther* 2022; **28**: 85.e1–85.e9.

12. Kobulnicky DJ, Sabo RT, Sharma S *et al*. The influence of lymphoid reconstitution kinetics on clinical outcomes in allogeneic stem cell transplantation. *Leuk Lymph* 2018; **59**: 2973–2981.

13. Meier J, Roberts C, Avent K *et al*. Fractal organization of the human T cell repertoire in health and after stem cell transplantation. *Biol Bl Mar Transpl* 2013; **19**: 366–377.

14. Meier JA, Haque M, Fawaz M *et al*. T cell repertoire evolution after allogeneic bone marrow transplantation: an organizational perspective. *Biol Bl Mar Transpl* 2019; **25**: 868–882.

15. Abdul Razzaq B, Scalora A, Koparde VN *et al*. Dynamical system modeling to simulate donor T cell response to whole exome sequencing-derived recipient peptides demonstrates different alloreactivity potential in HLA-matched and -mismatched donor-recipient pairs. *Biol Bl Mar Transpl* 2016; **22**: 850–861.

16. Koparde V, Abdul Razzaq B, Suntum T *et al*. Dynamical system modeling to simulate donor T cell response to whole exome sequencing-derived recipient peptides: understanding randomness in alloreactivity incidence following stem cell transplantation. *PLoS One* 2017; **12**: e0187771.

17. Nakamae H, Nakane T, Okamura H *et al*. A phase II study of post-transplant cyclophosphamide combined with tacrolimus for GVHD prophylaxis after HLA-matched related/unrelated allogeneic hematopoietic stem cell transplantation. *Int J Hematol* 2022; **115**: 77–86.

18. Meybodi MA, Cao W, Luznik L *et al*. HLA-haploidentical vs matched-sibling hematopoietic cell transplantation: a systematic review and meta-analysis. *Blood Adv* 2019; **3**: 2581–2585.

19. Rashidi A, Hamadani M, Zhang MJ *et al*. Outcomes of haploidentical vs matched sibling transplantation for acute myeloid leukemia in first complete remission. *Blood Adv* 2019; **3**: 1826–1836.

20. Portier DA, Sabo RT, Roberts CH *et al*. Anti-thymocyte globulin for conditioning in matched unrelated donor hematopoietic cell transplantation provides comparable outcomes to matched related donor recipients. *Bone Mar Transpl* 2012; **47**: 1513–1519.

21. Shiratori S, Kurata M, Sugita J *et al*. Graft-versus-host disease prophylaxis using low-dose antithymocyte globulin in peripheral blood stem cell transplantation-a matched-pair analysis. *Transpl Cell Ther* 2021; **27**: 995.e1–995.e6.

22. Baron F, Galimard JE, Labopin M *et al*. Allogeneic peripheral blood stem cell transplantation with anti-thymocyte globulin *versus* allogeneic bone marrow transplantation without anti-thymocyte globulin. *Haematologica* 2020; **105**: 1138–1146.

23. Lakkaraja M, Scordo M, Mauguen A *et al*. Antithymocyte globulin exposure in CD34$^+$ T-cell-depleted allogeneic hematopoietic cell transplantation. *Blood Adv* 2022; **6**: 1054–1063.

24. Bosch M, Dhadda M, Hoegh-Petersen M *et al*. Immune reconstitution after anti-thymocyte globulin-conditioned hematopoietic cell transplantation. *Cytotherapy* 2012; **14**: 1258–1275.

25. Admiraal R, Lindemans CA, van Kesteren C *et al*. Excellent T-cell reconstitution and survival depend on low ATG exposure after pediatric cord blood transplantation. *Blood* 2016; **128**: 2734–2741.

26. Toor A, Rodriguez T, Bauml M *et al*. Feasibility of conditioning with thymoglobulin and reduced intensity TBI to reduce acute GVHD in recipients of allogeneic SCT. *Bone Mar Transpl* 2008; **42**: 723–731.

27. Kharfan-Dabaja M, Mhaskar R, Reljic T *et al*. Mycophenolate mofetil versus methotrexate for prevention of graft-versus-host disease in people receiving allogeneic hematopoietic stem cell transplantation. *Cochrane Database Syst Rev* 2014; **7**: CD010280.

28. Storb R, Yu C, Wagner JL *et al*. Stable mixed hematopoietic chimerism in DLA-identical littermate dogs given sublethal total body irradiation before and pharmacological immunosuppression after marrow transplantation. *Blood* 1997; **89**: 3048–3054.

29. Mapara MY, Pelot M, Zhao G, Swenson K, Pearson D, Sykes M. Induction of stable long-term mixed hematopoietic chimerism following nonmyeloablative conditioning with T cell-depleting antibodies, cyclophosphamide, and thymic irradiation leads to donor-specific *in vitro* and *in vivo* tolerance. *Biol Bl Mar Transpl* 2001; **7**: 646–655.

30. Masson F, Mount AM, Wilson NS, Belz GT. Dendritic cells: driving the differentiation programme of T cells in viral infections. *Immunol Cell Biol* 2008; **86**: 333–342.

31. Conti L, Cardone M, Varano B, Puddu P, Belardelli F, Gessani S. Role of the cytokine environment and cytokine receptor expression on the generation of functionally distinct dendritic cells from human monocytes. *Eur J Immunol* 2008; **38**: 750–762.

32. Banchereau J, Steinman RM. Dendritic cells and the control of immunity. *Nature* 1998; **392**: 245–252.

33. Conti L, Gessani S. GM-CSF in the generation of dendritic cells from human blood monocyte precursors: recent advances. *Immunobiology* 2008; **213**: 859–870.

34. Choi D, Perrin M, Hoffmann S *et al*. Dendritic cell-based vaccines in the setting of peripheral blood stem cell transplantation: CD34+ cell-depleted mobilized peripheral blood can serve as a source of potent dendritic cells. *Clin Can Res* 1998; **4**: 2709–2716.

35. Ho VT, Mirza NQ, Junco DD, Okamura T, Przepiorka D. The effect of hematopoietic growth factors on the risk of graft-vs-host disease after allogeneic hematopoietic stem cell transplantation: a meta-analysis. *Bone Mar Transpl* 2003; **32**: 771–775.

36. Toor AA, Payne KK, Chung HM *et al*. Epigenetic induction of adaptive immune response in multiple myeloma: sequential azacitidine and lenalidomide generate cancer is antigen-specific cellular immunity. *Br J Haematol* 2012; **158**: 700–711.

37. Wang Y, Xiang Y, Xin VW *et al*. Dendritic cell biology and its role in tumor immunotherapy. *J Hematol Oncol* 2020; **3**: 107.

38. Toor AA, Sabo RT, Chung HM *et al*. Favorable outcomes in patients with high donor-derived T cell count after *in vivo* T cell-depleted reduced-intensity allogeneic stem cell transplantation. *Biol Bl Mar Transpl* 2012; **18**: 794–804.

39. Bensinger W, Stem Cell Trialists' Collaborative Group. Individual patient data meta-analysis of allogeneic peripheral blood stem cell transplant vs bone marrow transplant in the management of hematological malignancies: indirect assessment of the effect of day 11 methotrexate administration. *Bone Mar Transpl* 2006; **38**: 539–546.

40. de Koning C, Admiraal R, Nierkens S, Boelens JJ. Immune reconstitution and outcomes after conditioning with anti-thymocyte-globulin in unrelated cord blood transplantation; the good, the bad, and the ugly. *Stem Cell Investig* 2017; **4**: 38.

41. Admiraal R, Nierkens S, de Witte MA *et al*. Association between anti-thymocyte globulin exposure and survival outcomes in adult unrelated haemopoietic cell transplantation: a multicentre, retrospective, pharmacodynamic cohort analysis. *Lancet Haematol* 2017; **4**: e183–e191. Erratum in: Lancet Haematol. 2017; 4: e201.

42. Luznik L, O'Donnell PV, Symons HJ *et al*. HLA-haploidentical bone marrow transplantation for hematologic malignancies using nonmyeloablative conditioning and high-dose, posttransplantation cyclophosphamide. *Biol Bl Mar Transpl* 2008; **14**: 641–650.

43. Boyette LB, Macedo C, Hadi K *et al*. Phenotype, function, and differentiation potential of human monocyte subsets. *PLoS One* 2017; **12**: e0176460.

44. Chérel M, Choufi B, Trauet J *et al*. Naïve subset develops the most important alloreactive response among human CD4⁺ T lymphocytes in human leukocyte antigen-identical related setting. *Eur J Haematol* 2014; **92**: 491–496.

45. Eksioglu EA, Mahmood SS, Chang M, Reddy V. GM-CSF promotes differentiation of human dendritic cells and T lymphocytes toward a predominantly type 1 proinflammatory response. *Exp Hematol* 2007; **35**: 1163–1171.

46. de Koning C, Gabelich JA, Langenhorst J *et al*. Filgrastim enhances T-cell clearance by antithymocyte globulin exposure after unrelated cord blood transplantation. *Blood Adv* 2018; **2**: 565–574.

47. Orfali N, Zhang MJ, Allbee-Johnson M *et al*. Planned granulocyte colony-stimulating factor adversely impacts survival after allogeneic hematopoietic cell transplantation performed with thymoglobulin for myeloid malignancy. *Transpl Cell Ther* 2021; **27**: 993.e1–993.e8.

48. Afram G, Simón JAP, Remberger M *et al*. Reduced intensity conditioning increases risk of severe cGVHD: identification of risk factors for cGVHD in a multicenter setting. *Med Oncol* 2018; **35**: 79.

49. Bonifazi F, Rubio MT, Bacigalupo A *et al*. Rabbit ATG/ATLG in preventing graft-versus-host disease after allogeneic stem cell transplantation: consensus-based recommendations by an international expert panel. *Bone Mar Transpl* 2020; **55**: 1093–1102.

50. Dey BR, McAfee S, Colby C *et al*. Impact of prophylactic donor leukocyte infusions on mixed chimerism, graft-versus-host disease, and antitumor response in patients with advanced hematologic malignancies treated with nonmyeloablative conditioning and allogeneic bone marrow transplantation. *Biol Blood Mar Transpl* 2003; **9**: 320–329.

51. Zhang L, Rosenberger WF. Response-adaptive randomization for clinical trials with continuous outcomes. *Biometrics* 2006; **62**: 562–569.

52. Eisele JR. The doubly adaptive biased coin Design for Sequential Clinical-Trials. *J Stat Plan Infer* 1994; **38**: 249–261.

53. Immunoseq Adaptive Corp. Biotechnologies, immunoSEQ Assay: TCRB locus methods example. 2021. https://adaptivebiotech.showpad.com/share/zFRq5TBLXHzy6dzxZgEiZ

Supporting Information

Additional supporting information may be found online in the Supporting Information section at the end of the article.